J. Fluid Mech. (2001), *vol.* 435, *pp.* 289–303. Printed in the United Kingdom

Theoretical investigation of unsteady flow interactions with a premixed planar flame

By TIM LIEUWEN

School of Aerospace Engineering, Georgia Institute of Technology, Atlanta, GA 30332-0150, USA
e-mail: tim.lieuwen@aerospace.gatech.edu

(Received 21 January 2000 and in revised form 7 November 2000)

This paper presents the results of a theoretical study of the interactions between a laminar, premixed flame front and a plane acoustic wave. Its objective is to elucidate the processes that damp or drive acoustic waves as they interact with flames. Using linear analysis, the characteristics of the acoustic field, the flame's movement and wrinkling in response to acoustic perturbations, and the acoustic energy that is produced or dissipated at the flame are calculated. These calculations show that the net acoustic energy flux out of the flame is controlled by competing acoustic energy production and dissipation processes. Energy is added to the acoustic field by unsteady heat release processes resulting from the unsteady flux of unburned reactants through the flame by fluctuations in the flame speed or density of the unburned reactants. Energy is dissipated by the transfer of acoustic energy into fluctuations in vorticity that are generated at the flame front because of the misaligned fluctuating pressure and mean density gradients (i.e. the baroclinic vorticity production mechanism). The paper concludes by showing how these results can be generalized to determine the response of planar flames to an arbitrarily complex acoustic field. The principal contribution of this work is its demonstration that the excitation of vorticity and fluctuations in the flame speed have significant qualitative and quantitative affects on the interactions between flames and acoustic waves.

1. Introduction

This paper describes the results of an investigation of the interactions between a premixed flame front and plane acoustic waves. Its objective is to elucidate the processes that drive or damp acoustic waves as they interact with a flame. These interactions play an important role in the unsteady behaviour of many combustion systems, e.g. in the self-excited, combustion driven oscillations that occur in many combustors (Cohen & Anderson 1996; Lieuwen & Zinn 1998*a, b*).

Such interactions are inherently complex and involve simultaneous interactions between several flow and combustion processes. Such processes include: (i) wrinkling and movement of the flame front by the local velocity fluctuations accompanying the acoustic disturbance; (ii) fluctuations in the flame's local consumption rate (i.e. the flame speed) by the pressure, temperature, and strain rate fluctuations; (iii) reflection and refraction of acoustic waves as they encounter the sudden change in temperature and acoustic impedance of the gas at the flame front; (iv) creation of a complex, three-dimensional local acoustic wave field by the superposition of incident and scattered waves from the flame front; (v) excitation of rotational disturbances (i.e. vorticity fluctuations) by the purely dilatational acoustic disturbances when they encounter the flame (through the baroclinic vorticity production mechanism); and (vi) modulation of intrinsic flame instabilities.

Owing to the complex nature of these interactions, our current understanding of them is incomplete. Several analyses in the literature, however, have made important contributions to their current understanding. The paragraph below briefly summarizes these analyses. Since flame fronts are significantly thinner than acoustic wavelengths over most frequencies of interest, we discuss only those studies that limited their attention to the response of a thin flame front, i.e. where the flame was treated as a surface of discontinuity. Analyses of high-frequency excitation and the effects of acoustic forcing on the flame structure are not considered in this paper; see McIntosh (1991) and references therein for treatments of this subject.

Chu appears to have been the first to study the response of a thin flame front to an acoustic disturbance (Chu 1953). His one-dimensional analysis considered the response of an infinitely long flame to normally impinging acoustic waves. The resultant acoustic field was determined by applying conservation and kinematical matching conditions across the flame. A significant result of this study was its demonstration that acoustic waves could be excited or amplified by flames. Because Chu only considered one-dimensional interactions, the effects of flame movement back and forth were considered in this analysis, but two-dimensional effects, such as flame wrinkling or vorticity production were not.

Chu's work was extended to model the flame dynamics in realistic combustor geometries by Marble & Candel (1978), Subbaiah (1983), Poinsot & Candel (1988), and Yang & Culick (1983). These investigations analysed the interactions between acoustic waves and a flame stabilized in a combustor with a two-dimensional mean flow field (e.g. a ramjet or gas turbine). The acoustic field was assumed to be one-dimensional or quasi-one-dimensional. A significant result of these studies was their demonstration that the maximum amplification of acoustic waves by the flame occurred at certain values of the flame Strouhal number, $St = fL_{flame}/\bar{u}$, where f and $\bar{u}$ denote the frequency and axial mean velocity. Since the quantity $L_{flame}/\bar{u}$ describes the amount of time required for a disturbance to convect along the flame at the flow speed, these results showed that the flame amplified disturbances with acoustic periods $T = 1/f$ that matched particular multiples of the characteristic convective time. Thus, these studies clearly showed the importance of considering a finite flame region in modelling the interactions between acoustic waves and a flame. Similar models have been considered more recently by Fleifel *et al.* (1996), Peracchio & Proscia (1998) and Dowling (1997).

Because of the complex nature of the modelled phenomenon, several chemical and physical processes were neglected in these analyses. For example, with the exception of Chu (1953) and Poinsot & Candel (1988) these studies did not account for fluctuations in the local flame speed. Also, none of these studies considered the effects of two- or three-dimensional acoustic oscillations or the excitation of vorticity at the flame by acoustic waves. Of course, it is clear that in order for these analyses to retain analytical tractability, some simplifications are necessary. However, given the current level of understanding of these interactions, it is unclear whether these studies retained or neglected the dominant processes.

In order to clarify our current understanding of the dominant processes controlling flame–acoustic wave interactions, this paper describes a fundamental study of the response of an idealized, model flame configuration to acoustic disturbances. Although the investigated geometry does not resemble flames in any practical configuration,

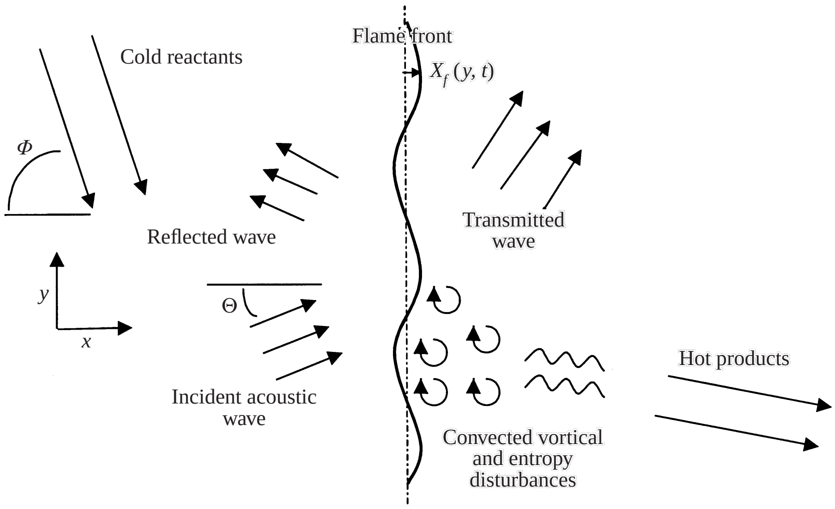

FIGURE 1. Schematic of the investigated geometry.

its simplicity allows analytical tractability and, thus, simultaneous examination of such effects as fluctuations in flame consumption rate and vorticity production in a two-dimensional acoustic field.

This paper is organized in the following manner. The next section discusses the assumptions of the study, presents solutions for the unsteady wave motions up and downstream of the flame, and illustrates typical time dependences of the velocity and flame position. Then, the conditions under which acoustic energy is produced or dissipated at the flame are analysed. Finally, the important conclusions of this analysis are presented and generalizations of this study and recommendations for further research are discussed.

2. Analysis and results

The investigated problem is shown in figure 1. A thin, infinitely long, laminar flame nominally at $x = 0$ separates uniform regions of cold reactants and hot products. The flame is excited by a plane acoustic wave that is inclined at an angle of Θ to the horizontal.

The following assumptions are made about these regions and the flame to simplify the analysis: (i) the flame has a thickness, d, which is much smaller than an acoustic wavelength; (ii) chemical time scales are much shorter than the acoustic period, T (i.e. $\tau_{chem} \ll T$); (iii) the regions outside the flame are isentropic, i.e. $\mathrm{D}s/\mathrm{D}t = 0$; (iv) the mean flow field is uniform, isothermal, has a low Mach number, M, and is composed of a calorically perfect gas; (v) the ratio of the flame speed and mean flow speed, $\eta = S/\bar{u}$, is small; (vi) molecular transport effects are negligible; and (vii) all disturbances are infinitesimal in magnitude. Since the Mach number, M, the ratio of the flame and mean flow speed, η (thus, the flame speed Mach number equals $M\eta$), and the ratio of the flame thickness and the acoustic wavelength, d/λ, are assumed to be small, all effects of $O(kd = 2\pi d/\lambda)$, and of higher order than $O(M\eta)$ (e.g. $O(M^2\eta)$ or $O(M\eta)^2$) are neglected in this analysis, where $k = \omega/c$ is the acoustic wavenumber. Also, assuming that τ_{chem} is of the order of the ratio of the flame thickness and flame speed, i.e. $\tau_{chem} \sim d/S$, all terms of $O(\tau_{chem}/T \sim fd/S = kd/(2\pi M\eta)) \sim O(kd/M\eta)$ are neglected, see assumption (ii).

Given the above assumptions, the equations describing the flow fields on either side of the flame front are described by the familiar Euler equations and the energy equation stating that $\mathrm{D}s/\mathrm{D}t = 0$. The linear analysis below employs the standard practice of decomposing these equations into systems of steady and unsteady ones by writing each dependent variable as a sum of its mean and fluctuating component (e.g. $p = \bar{p} + p'$) and neglecting second-order terms in perturbations. It should be noted that the disturbance quantities can be decomposed into three canonical modes of disturbance (Chu & Kovasnay 1958). That is, a disturbance field can be expressed as a summation of disturbances arising from fluctuations in vorticity, entropy, and volume (i.e. acoustic), e.g. $p' = p'_a + p'_v + p'_s$. Acoustic disturbances propagate with a characteristic velocity equal to the speed of sound, while vorticity and entropy disturbances are convected with the mean flow velocity.

Assuming that the unsteady fields are forced by a harmonically oscillating plane wave at a frequency of $\omega = k\bar{c}$ incident at an angle of $\Theta = \sin^{-1} n_y$, the following solutions for the disturbance quantities can be determined using standard techniques:

Pressure

$$\frac{p'}{\bar{p}} = (D^+ \mathrm{e}^{\mathrm{i}k\beta^+ x} + D^- \mathrm{e}^{\mathrm{i}k\beta^- x})\mathrm{e}^{\mathrm{i}kny}\mathrm{e}^{-\mathrm{i}\omega t}, \tag{1}$$

x-velocity component

$$\frac{u'}{\bar{c}} = \frac{1}{\gamma}(D^+ n_x^+ \mathrm{e}^{\mathrm{i}k\beta^+ x} + D^- n_x^- \mathrm{e}^{\mathrm{i}k\beta^- x} - \frac{nM_x}{1 - nM_y} V_v \mathrm{e}^{\mathrm{i}kx(1-nM_y)/M_x})\mathrm{e}^{\mathrm{i}kny}\mathrm{e}^{-\mathrm{i}\omega t}, \tag{2}$$

y-velocity component

$$\frac{v'}{\bar{c}} = \frac{1}{\gamma}(D^+ n_y^+ \mathrm{e}^{\mathrm{i}k\beta^+ x} + D^- n_y^- \mathrm{e}^{\mathrm{i}k\beta^- x} + V_v \mathrm{e}^{\mathrm{i}kx(1-nM_y)/M_x})\mathrm{e}^{\mathrm{i}kny}\mathrm{e}^{-\mathrm{i}\omega t}, \tag{3}$$

density

$$\frac{\rho'}{\bar{\rho}} = \frac{1}{\gamma}(D^+ \mathrm{e}^{\mathrm{i}k\beta^+ x} + D^- \mathrm{e}^{\mathrm{i}k\beta^- x} + \rho_s \mathrm{e}^{\mathrm{i}kx(1-nM_y)/M_x})\mathrm{e}^{\mathrm{i}kny}\mathrm{e}^{-\mathrm{i}\omega t}, \tag{4}$$

where

$$\beta^{\pm} = \frac{-M_x(1 - nM_y) \pm \sqrt{(1 - nM_y)^2 - n^2(1 - M_x^2)}}{1 - M_x^2} \tag{5}$$

and

$$n_y^{\pm} = \frac{n}{1 - nM_y - \beta^{\pm} M_x}, \quad n_x^{\pm} = \pm\sqrt{1 - (n_y^{\pm})^2}, \tag{6}$$

and where γ, p, ρ, u, v, and c denote the ratio of specific heats, pressure, density, x-velocity component, y-velocity component, and speed of sound, respectively. The quantities n_x and n_y denote the x- and y-directions of propagation of the acoustic wave in the absence of mean flow. They are related to the quantity n, which appears in (1)–(4), through (5) and (6). The superscripts $+/-$ refer to disturbances propagating in the $+/-$ x-direction, respectively. The subscripts x and y denote the x- and y-components of the disturbance, respectively. Finally, the quantities V_v, ρ_s, D^+, and D^- denote the magnitudes of the vortical velocity, 'entropic' density, and rightward and leftward propagating acoustic disturbances, respectively. These acoustic, vorticity, and entropy disturbances propagate independently in the linear approximation (Chu & Kovasnay 1958), although they are coupled at the flame.

Equations (1)–(6) describe the unsteady flow fields on the up- and downstream sides of the flame. The magnitudes and phases of these waves (e.g. V_v, ρ_s, D^+, and D^-) are determined with kinematical equations for the flame position and matching conditions that couple the flow fields up and downstream of the flame front. These equations are given in Markstein (1964) and other references and are not reproduced here. Employing a similar linearization procedure to these equations as described above and neglecting terms of $O(M\eta)^2$ yields the following interface conservation conditions that relate the values of the disturbance quantities across the flame, where the subscripts 1 and 2 denote the value of the variable on the up- and downstream sides of the flame:

mass

$$\frac{\rho_1'}{\bar{\rho}_1} + \frac{S_1'}{\bar{S}_1} = \frac{\rho_2'}{\bar{\rho}_2} + \frac{S_2'}{\bar{S}_2}, \tag{7}$$

normal momentum

$$\frac{p_1'}{\bar{p}} - \frac{p_2'}{\bar{p}} = 2\gamma M_{x1}\left(\sqrt{\Lambda}\frac{u_2'}{\bar{c}_2} - \frac{u_1'}{\bar{c}_1}\right), \tag{8}$$

tangential momentum

$$\frac{v_1'}{\bar{c}_1} - \sqrt{\Lambda}\frac{v_2'}{\bar{c}_2} + (\Lambda - 1)nM_{x1}\frac{u_1'}{\bar{c}_1} = 0, \tag{9}$$

energy

$$\gamma\sqrt{\Lambda}\frac{u_2'}{\bar{c}_2} - \gamma\frac{u_1'}{\bar{c}_1} + M_{x1}\left(\gamma\Lambda\frac{p_2'}{\bar{p}} - (\gamma + \Lambda - 1)\frac{p_1'}{\bar{p}} - \gamma(\Lambda - 1)\frac{S_1'}{\bar{S}_1}\right) = 0, \tag{10}$$

flame front equations

$$k_1 X_f' = \mathrm{i}\frac{(u_1'/\bar{c}_1) - M_{x1}(S_1'/\bar{S}_1)}{1 - nM_{y1}}, \tag{11}$$

$$\Lambda M_{x1}\frac{S_2'}{\bar{S}_2} = \sqrt{\Lambda}\frac{u_2'}{\bar{c}_2} - \frac{u_1'}{\bar{c}_1} + M_{x1}\frac{S_1'}{\bar{S}_1}, \tag{12}$$

where θ, Λ, X_f and h denote the temperature, mean temperature jump across the flame (i.e. $\Lambda = \bar{\theta}_2/\bar{\theta}_1$), flame position (defined by the equation $x - X_f(y,t) = 0$), and enthalpy, respectively. Note that, as in (1)–(6), all variables have an $\mathrm{e}^{\mathrm{i}kny}$- and $\mathrm{e}^{\mathrm{i}\omega t}$-$y$-direction and time dependence, respectively.

Similarly, after neglecting terms of $O(M\eta)^2$, algebraic manipulation of the corresponding equations for the mean quantities yields the relations $\bar{\rho}_1\bar{S}_1 = \bar{\rho}_2\bar{S}_2$, $\bar{p}_1 = \bar{p}_2 \equiv \bar{p}$, $\bar{v}_1 = \bar{v}_2 \equiv \bar{v}$, $\bar{h}_2 = \bar{h}_1 \equiv \bar{h}$, and $\bar{X}_f = 0$.

Equations (7)–(12) can be further simplified. First, substitution of (10) into the right-side of (8) shows that the fluctuating pressure difference across the flame is $O(M_x^2) = O(M\eta)^2$. Thus, to the order of approximation of this analysis

$$\frac{p_1'}{\bar{p}} = \frac{p_2'}{\bar{p}} \equiv \frac{p'}{\bar{p}}. \tag{13}$$

Utilizing (13), equation (10) can be written as

$$\gamma\sqrt{\Lambda}\frac{u_2'}{\bar{c}_2} - \gamma\frac{u_1'}{\bar{c}_1} + (\Lambda - 1)M_{x1}\left((\gamma - 1)\frac{p'}{\bar{p}} - \gamma\frac{S_1'}{\bar{S}_1}\right) = 0. \tag{14}$$

Utilizing (12) and (13), equation (7) can be written as

$$\frac{\rho_2'}{\bar{\rho}_2} = \frac{\rho_1'}{\bar{\rho}_1} + \frac{(\Lambda - 1)(\gamma - 1)}{\Lambda\gamma}\frac{p'}{\bar{p}}. \tag{15}$$

An expression for S_1' is needed to couple the flame chemistry with the unsteady fields. In general, the flame speed is a function of the local pressure, temperature, reactant composition, and flame strain rate (Clavin 1985; Metghalchi & Keck 1982). Since the modelled configuration is planar (i.e. has an infinite mean radius of curvature), the leading-order effects of flame wrinkling and flow distortion by acoustic flow disturbances upon the flame speed due to unsteady flame strain are of $O(kd)$ and $O(kd/M\eta)$, respectively, and are, thus, neglected (see assumptions (i) and (ii)†). Also, since this study is investigating the response of the flame to acoustic disturbances, the reactive mixture is assumed to have a constant composition. Under these conditions, the fluctuating flame speed is only a function of the instantaneous value (see assumption (i)) of the pressure and temperature, i.e. $S_1 = f(p_1, T_1)$. Linearizing this expression yields

$$\frac{S_1'}{\bar{S}_1} = \kappa_p\frac{p'}{\bar{p}} + \kappa_T\frac{T_1'}{\bar{T}_1}. \tag{16}$$

Since the upstream conditions are isentropic, i.e. $T_1 = f(p_1)$, equation (16) can be written as

$$\frac{S_1'}{\bar{S}_1} = \left(\kappa_p + \frac{\gamma - 1}{\gamma}\kappa_T\right)\frac{p'}{\bar{p}} = \kappa\frac{p'}{\bar{p}}. \tag{17}$$

The values of the constants in (17) can be determined from an analysis of the flame structure that includes chemical kinetics, e.g. see McIntosh (1991) or Clavin (1985). Alternatively, the constants can be evaluated approximately by determining the dependence of the mean flame speed upon the mean pressure and temperature using experimental data (consistent with assumption (ii), this approximation assumes a quasi-steady change of the flame speed with changes in pressure and temperature), i.e. using the empirical relationship for the flame speed, $S \propto p^{n_p}T^{n_T}$, the flame speed response parameter, κ, is

$$\kappa = \left(n_p + \frac{\gamma - 1}{\gamma}n_T\right). \tag{18}$$

In order to estimate typical values of the flame speed response parameter for laminar flames, the parameters n_p and n_T in (18) were determined from Metghalchi & Keck's (1982) data. Their data suggests that typical values of κ for hydrocarbon flames fall in the $0.4 < \kappa < 0.5$ range.

Solutions

Equations (9), (12)–(15) and (17) are a set of algebraic equations for p', u', v', ρ', and S'. In order to determine these quantities, it is necessary to determine the amplitudes of the reflected and transmitted acoustic waves and the convected vortical and entropy waves (e.g. V_v or D^+, see (1)–(4)). By substituting the expression for p', u', and v' in (1)–(3) into (9) and (3)–(15), the following leading-order (i.e. neglecting all terms of $O(M)$ and higher) solutions for the disturbance wave amplitudes are obtained:

† It can be shown that the calculated acoustic energy produced or dissipated at the flame remains unchanged even if assumption (ii) were relaxed and the leading $O(kd/M\eta)$ flame strain effects were retained. Inclusion of these $O(kd/M\eta)$ flame strain effects introduces terms of the form $p'\mathrm{d}p'/\mathrm{d}t$ in the expression for the acoustic energy flux, a term whose time average is zero.

incident disturbance upstream ($D_1^+ = 1, D_2^- = 0, V_{v1} = 0, \rho_{s1} = 0$)

$$\left.\begin{aligned} D_2^+ &= \frac{2}{1+\sqrt{\Lambda(1-\Lambda\sin^2\Theta)/(1-\sin^2\Theta)}}, \quad D_1^- = D_2^+ - 1, \\ V_{v2} &= \frac{(1-\Lambda)\sin\Theta}{\sqrt{\Lambda}}D_2^+, \quad \rho_{s2} = \frac{(\Lambda-1)(\gamma-1)}{\Lambda}D_2^+. \end{aligned}\right\} \tag{19}$$

incident disturbance downstream ($D_2^- = 1, D_1^+ = 0, V_{v1} = 0, \rho_{s1} = 0$)

$$\left.\begin{aligned} D_1^- &= \frac{2}{1+\sqrt{(1-(\sin^2\Theta)/\Lambda))/(\Lambda(1-\sin^2\Theta))}}, \quad D_2^+ = D_1^- - 1, \\ V_{v2} &= \frac{(1-\Lambda)\sin\Theta}{\Lambda}D_1^-, \quad \rho_{s2} = \frac{(\Lambda-1)(\gamma-1)}{\Lambda}D_1^-. \end{aligned}\right\} \tag{20}$$

These solutions describe the characteristics of the local disturbance field and flame position. Figure 2 plots particle pathlines for a number of incident acoustic wave angles, Θ, where the net particle drift from the mean flow is neglected. Corresponding plots of instantaneous particle streamlines and the flame position at one phase of the cycle (i.e. $\omega t = 0, 2\pi, \ldots$) are shown in figure 3.

In interpreting the results shown in figures 2 and 3, it is important to note the presence of a 'cutoff' angle for disturbances incident from upstream, i.e. a disturbance with an angle of incidence that is greater than $\Theta = \sin^{-1}(c_1/c_2) = \sin^{-1}(1/\Lambda)^{0.5}$ does not transmit acoustic energy through the flame, e.g. if $\Lambda = 8$, $\Theta_{cutoff} \sim 20°$. This cutoff phenomenon is well known in acoustics and optics and occurs when a disturbance propagates from a medium of lower to higher sound speed. There is a discontinuous change in the characteristics of the acoustic field when Θ is just above and below this angle. The same phenomenon does not occur when the disturbance is incident from downstream because, in this case, energy is transmitted through the flame for all angles of incidence.

Examination of figures 2 and 3 shows that the acoustic field upstream of the flame resembles that typically observed in analyses of acoustic wave reflection off of locally reacting surfaces or membranes (Pierce 1991). The acoustic field downstream of the flame is quite different, however, due to the vortical velocity fluctuations that are superimposed on the acoustic fluctuations. These vortical velocity fluctuations are primarily in the y-direction and their presence is most pronounced when Θ is above the cutoff angle, i.e. at $\Theta = 40°$. At these incident angles, the transmitted acoustic wave is damped as it propagates away from the flame, and the fluctuating velocity on the downstream side of the flame is dominated by the vorticity mode. For waves incident from downstream, i.e. $\Theta = 110$ and $\Theta = 150°$, no such cutoff phenomenon occurs and acoustic energy is transmitted for all incident angles. The figures show that, in both cases, the pathlines and streamlines on the downstream side of the flame exhibit complex behaviour due to the superposition of the acoustic wave and the convected vorticity wave.

3. Acoustic energy production by the flame

The energy exchange between the unsteady motions and the flame significantly affects the overall unsteady behaviour of the system. Thus, a great deal of insight into the global effects of flame–acoustic wave interactions on the unsteady behaviour

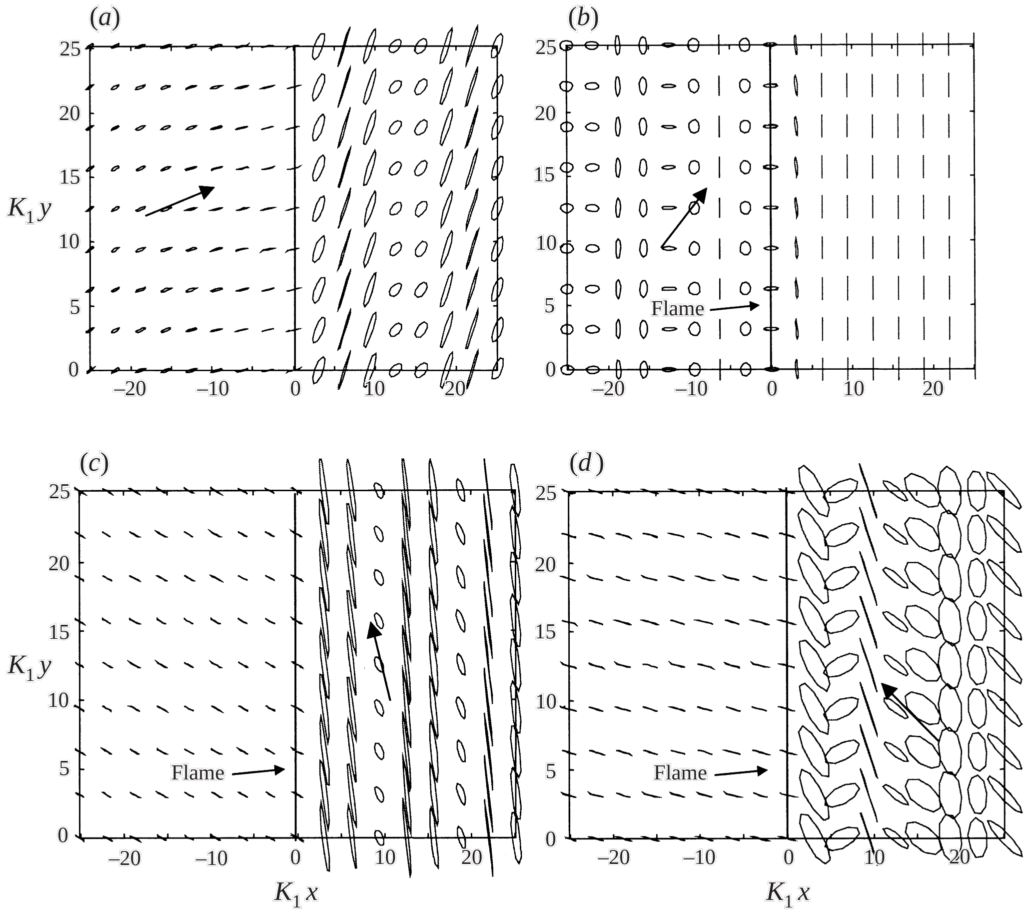

FIGURE 2. Particle pathlines for several angles of wave incidence ($\Lambda = 8$). (*a*) $\Theta = 15°$, (*b*) $\Theta = 40°$, (*c*) $\Theta = 110°$, (*d*) $\Theta = 150°$.

of combustion systems can be obtained by examining the energy flux into and out of the flame, $\boldsymbol{I} \cdot \boldsymbol{n}_{flame}$. The mean flux of acoustic energy due to unsteady motions can be written as (Pierce 1991; Lieuwen 1999)

$$\langle \boldsymbol{I}_a \rangle = \left\langle \left(\frac{p'_a}{\bar{c}^2} \bar{\boldsymbol{u}} + \bar{\rho} \boldsymbol{u}'_a \right) \left(\frac{p'_a}{\bar{\rho}} + \bar{\boldsymbol{u}} \cdot \boldsymbol{u}'_a \right) \right\rangle, \tag{21}$$

where $\boldsymbol{I}_a$ is the acoustic energy flux. For compactness, the variables are written in non-dimensional form, i.e. $p'/\bar{p} \rightarrow \tilde{p}', \gamma u'/\bar{c} \rightarrow \tilde{u}', \gamma v'/\bar{c} \rightarrow \tilde{v}', \gamma S'/\bar{S} \rightarrow \tilde{S}', \gamma \langle \Delta \boldsymbol{I} \cdot \boldsymbol{n}_{flame} \rangle / \bar{p}_1 \bar{c}_1 \rightarrow \langle \Delta \boldsymbol{I} \rangle$. Using the expression for the net rate of acoustic energy production or dissipation at the flame, $\langle \Delta I \rangle = \langle$flux of energy out of flame$\rangle - \langle$flux of energy into flame$\rangle$, (21) can be written as (neglecting terms of higher-order than $O(M\eta)$)

$$\langle \Delta \boldsymbol{I}_a \rangle = \sqrt{\Lambda} \tilde{p}'_{2a} \tilde{u}'_{2a} - \tilde{p}'_{1a} \tilde{u}'_{a1} + \sqrt{\Lambda} M_{x2} \tilde{p}'^2_{2a} - M_{x1} \tilde{p}'^2_{1a}$$
$$+ \sqrt{\Lambda} \tilde{u}'_{2a} (M_{x2} \tilde{u}'_{2a} + M_{y2} \tilde{v}'_{2a}) - \tilde{u}'_{1a} (M_{x1} \tilde{u}'_{1a} + M_{y1} \tilde{v}'_{1a}). \tag{22}$$

Equation (22) can be simplified with the matching conditions in (9) and (13)–(15)

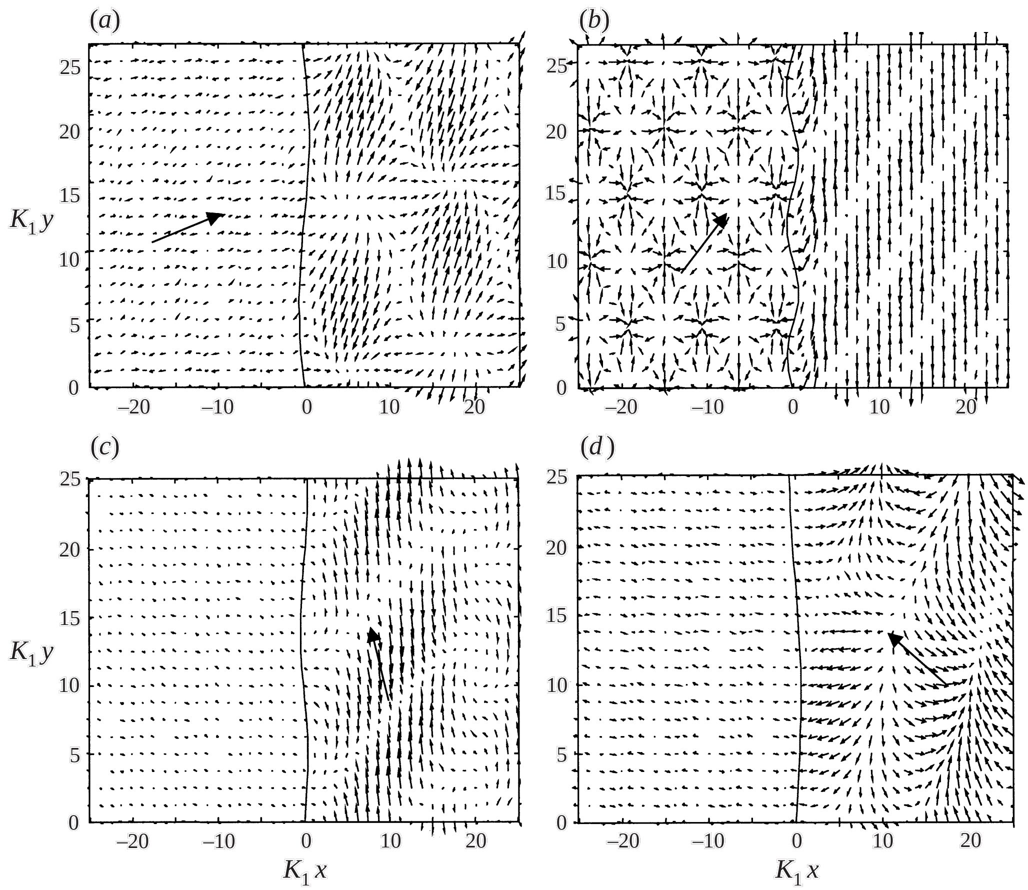

FIGURE 3. Instantaneous (i.e. at $\omega t = 0, 2\pi, \ldots$) velocity vectors and flame location for the same conditions as in figure 2.

and the acoustic solutions in (1)–(4). For example, using (13) and (14), the first two terms in (22) can be written as

$$\sqrt{\Lambda}\tilde{p}'_{2a}\tilde{u}'_{2a} - \tilde{p}'_{1a}\tilde{u}'_{a1} = -(\Lambda - 1)M_{x1}\tilde{p}'((\gamma - 1)p' - S'_1) - \sqrt{\Lambda}\tilde{u}'_{2v}\tilde{p}'. \quad (23)$$

In the same manner, the last four terms in (22) can be shown to be of higher order than $O(M\eta)$, and are neglected. The resulting expression for the acoustic energy flux is

$$\langle \Delta \tilde{I}_a \rangle = (\Lambda - 1)M_{x1}((2 - \gamma)|\tilde{p}'|^2 + \tilde{p}S'_1) - \sqrt{\Lambda}\tilde{u}'_{2v}\tilde{p}'. \quad (24)$$

Equation (24) shows that flame speed fluctuations only add energy to the acoustic field when the magnitude of the phase between S'_1 and p' is less than 90°. It should be emphasized that this result was derived without any *a priori* assumptions about the dependence of the flame speed upon the unsteady field.

Equation (24) is further simplified by substituting the results from (1)–(4), (17), (19) and (20) into (24) to obtain the following final result for the net energy flux flame out of the flame, normalized by the energy flux in the incident wave:

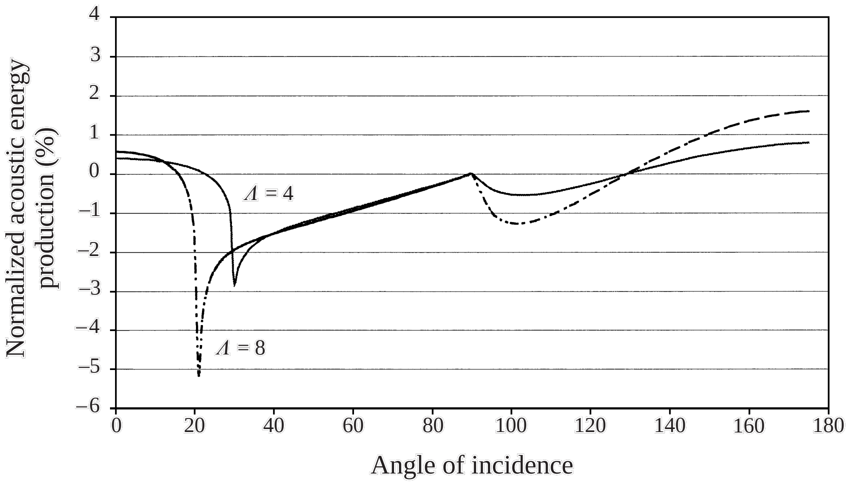

FIGURE 4. Dependence of normalized acoustic energy production by the flame, $\langle \Delta I_a \rangle / \langle I_{a,incident} \rangle$, upon the angle of incidence of the exciting disturbance ($\kappa = 0$, $M_{x1} = 0.005$, $\gamma = 1.4$).

wave incident from upstream ($0 < \Theta < 90$)

$$\frac{\langle \Delta I_a \rangle}{\langle I_{a,incident} \rangle} = \frac{4(\Lambda - 1)M_{x1}}{\left|1 + \sqrt{\Lambda(1 - \Lambda \sin^2\Theta)/(1 - \sin^2\Theta)}\right|^2} \frac{(2 - \gamma + \gamma\kappa - \Lambda \sin^2\Theta)}{\sqrt{(1 - \sin^2\Theta)}}, \tag{25}$$

wave incident from downstream ($90 < \Theta < 180$)

$$\frac{\langle \Delta I_a \rangle}{\langle I_{a,incident} \rangle} = \frac{4(\Lambda - 1)M_{x1}}{\left|1 + \sqrt{(1 - \sin^2\Theta/\Lambda)/\Lambda(1 - \sin^2\Theta)}\right|^2} \frac{(2 - \gamma + \gamma\kappa - \sin^2\Theta)}{\sqrt{\Lambda(1 - \sin^2\Theta)}}. \tag{26}$$

Equations (25) and (26) are the principal results of this study and explicitly show that the energy produced by the interaction of an acoustic wave with a flame depends upon the angle of the incident wave, $\Theta = \sin^{-1}(n_{yi})$, the flame speed Mach number, $M_{x1} = M\eta$, the temperature jump across the flame, Λ, the ratio of specific heats, γ, and the flame speed response parameter, κ. The ensuing paragraphs discuss the dependence of the acoustic energy upon these parameters.

Figure 4 illustrates the dependence of the acoustic energy flux out of the flame upon Θ for two different values of Λ. It shows that net acoustic energy is produced at normal incidence (i.e. $\Theta = 0$ or $180°$), consistent with Chu's (1953) prior results. The amount of acoustic energy that is produced decreases as the angle of incidence increases, however, and actually becomes negative (i.e. acoustic waves are damped) at $\Theta \approx 19°$ and $130°$ for $\Lambda = 8$. As discussed later, this damping arises from the transfer of energy from the acoustic mode to the vortical mode. The net intensity flux is zero for the degenerate case $\Theta = 90°$ where the incident wave is parallel to the flame.

Figure 5 illustrates the additional affects of flame speed modulation (i.e. $\kappa \neq 0$) on the acoustic energy flux out of the flame. The figure shows that flame speed fluctuations significantly affect the amount of acoustic energy that is produced at the flame. For example, net acoustic energy is produced over a wider range of angles as κ increases. The figure also shows that the combined effects of refraction, vorticity production and flame speed modulation produce a complex pattern of acoustic energy amplification/damping. For example, note the spike in acoustic energy production at

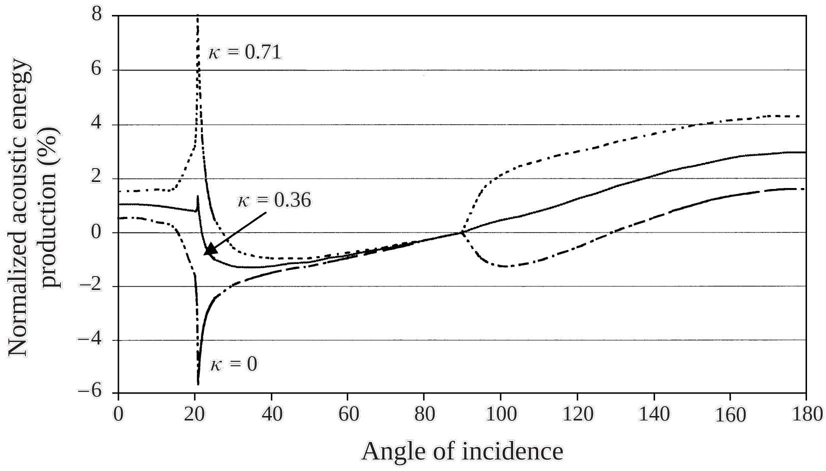

FIGURE 5. Dependence of normalized acoustic energy production by the flame, $\langle \Delta I_a \rangle / \langle I_{a,incident} \rangle$, upon the angle of incidence of the exciting disturbance ($M_{x1} = 0.005$, $\gamma = 1.4$, $\Lambda = 8$).

$\Theta \approx 20^\circ$ for the values $\kappa = 0.36$ and 0.71, before the wave becomes damped at higher angles of incidence. The discontinuous behaviour of the energy flux in the vicinity of this angle is due to the wave cutoff phenomenon discussed in the context of figures 2 and 3. Figure 5 also shows that waves incident from downstream are amplified at any angle for the values $\kappa = 0.36$ and $\kappa = 0.71$.

Consider further the conditions under which net acoustic energy is produced or damped. In the simplest case where the incident disturbance is normal to the flame (i.e. $\Theta = 0$ or 180°) equations (25 and 26) show that net acoustic energy is produced as long as $2 - \gamma + \gamma\kappa > 0$. Since γ is typically in the range $1.3 < \gamma < 1.4$ and the flame speed response parameter appears to always be positive, i.e. $\kappa > 0$, it follows that $2 - \gamma + \gamma\kappa$ is positive and, thus, the results of this analysis indicate that *normal acoustic–flame interactions always generate acoustic energy*.

Next, consider the case where the incident disturbance is oblique to the flame front, i.e. $\sin\Theta \neq 0$. The terms $-\Lambda \sin^2\Theta$ and $-\sin^2\Theta$ in the numerators of (25) and (26), respectively, arise from the excitation of vorticity and indicate its role in these interactions, i.e. *the excitation of vorticity by acoustic waves always acts as a source of acoustic damping*. Furthermore, figures 4 and 5 show that this damping may be significant enough to cause the terms $2 - \gamma + \gamma\kappa - \Lambda \sin^2\Theta$ or $2 - \gamma + \gamma\kappa - \sin^2\Theta$ in these equations to become negative above a certain 'critical' angle of incidence. This 'critical' angle is given by:

disturbance incident from upstream, downstream

$$\Theta_{crit} = \sin^{-1}\sqrt{\frac{2 - \gamma + \gamma\kappa}{\Lambda}}, \quad \sin^{-1}\sqrt{2 - \gamma + \gamma\kappa}. \tag{27}$$

Equation (27) indicates that a critical angle does not exist for some κ, Λ, γ combinations. In these instances, acoustic energy is produced for all angles of incidence. The expressions below quantify the conditions for which acoustic waves are only amplified by flames:

disturbance incident from upstream, downstream

$$\kappa > (\Lambda + \gamma - 2)/\gamma, \quad \kappa > (\gamma - 1)/\gamma. \tag{28}$$

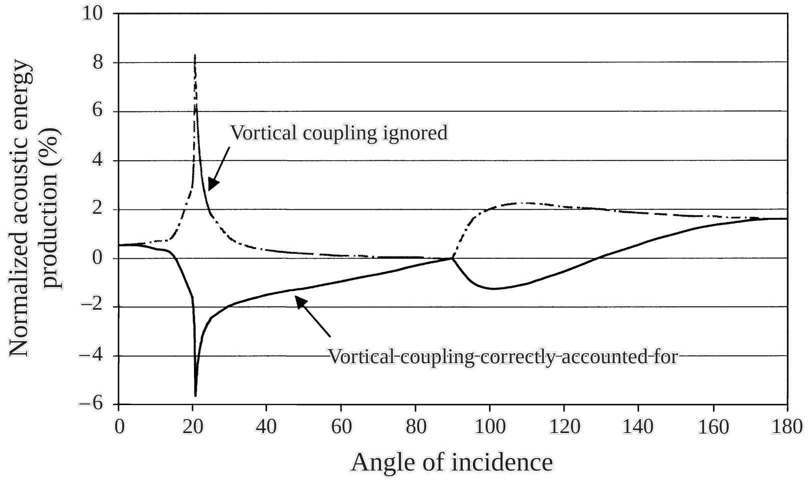

FIGURE 6. Dependence of normalized acoustic energy production by the flame, $\langle \Delta I_a \rangle / \langle I_{a,incident} \rangle$, upon the angle of incidence of the exciting disturbance when excitation of vorticity is and is not accounted for ($\kappa = 0$, $M_{x1} = 0.005$, $\gamma = 1.4$, $\Lambda = 8$).

Assuming values of $\gamma = 1.4$ and $4 < \Lambda < 8$, equation (28) indicates that acoustic energy is always produced by flame–acoustic wave interactions if $\kappa > 2.4$–5.3 for upstream incident waves and $\kappa > 0.29$ for downstream incident waves. Since, as discussed preciously, κ takes values of approximately $\kappa = 0.4$–0.5 in laminar hydrocarbon flames (based upon the data in Metghalchi & Keck 1982), it appears that *acoustic waves incident from upstream are always damped for some angles of incidence and acoustic waves incident from downstream are amplified for all angles of incidence.*

The role of vorticity production is next examined more closely. Its important role in flame–acoustic wave interactions can be understood by comparing the acoustic energy production that is calculated when the vorticity and acoustic coupling is ignored (i.e. the vortical velocity component in (2) and (3) is neglected) and when it is properly accounted for, see figure 6. (Neglecting vorticity production is equivalent to neglecting the $-\Lambda \sin^2 \Theta$ and $-\sin^2 \Theta$ terms in (25) and (26).) Figure 6 clearly shows that the two calculations produce qualitatively different results, e.g. acoustic energy is produced for all angles of incidence when the vortical–acoustic coupling is neglected. This figure shows that analyses of flame–acoustic interactions that neglect the excitation of vorticity significantly overestimate the amplification of acoustic waves by flames. It should be emphasized that the damping of acoustic waves that occurs because of baroclinic vorticity production at the flame does not imply that the overall energy in the unsteady motions is damped. Rather, it reflects the transfer of energy from the acoustic mode to the vorticity mode.

Reference to (25) and (26) or figure 6 indicates that two competing processes determine the ‘resultant’ energy flux out of the flame. The first process is the energy added to the acoustic field by the unsteady heat release, with a magnitude illustrated by the ‘Vortical coupling ignored’ curve in figure 6. Physically, this energy addition process is due to the unsteady flux of unburned reactants through the flame by either fluctuations in the flame speed or density of the unburned reactants. The second competing process is the damping of acoustic waves that arises from the transfer of acoustic energy into the vorticity mode. The net affect of these two competing processes is given by the ‘vortical coupling correctly accounted for’ curve in figure 6.

These competing mechanisms are the two key processes that are responsible for driving/damping acoustic oscillations in this model problem. Note, however, that other competing processes are likely to be present in realistic situations. For example, flame area fluctuations play no role in this problem but are likely to affect these interactions in reality. The critical angle, Θ_{crit}, refers to the angle at which the acoustic energy addition and dissipation by these competing processes balance. That is, above or below Θ_{crit}, one of the processes dominates.

The amount of acoustic damping provided by the excitation of vorticity is equal to the difference between the two curves in figure 6. For the parameter values used in this figure, this difference is as large as 14%, indicating that up to 14% of the energy in an incident acoustic wave is transferred into fluctuations in vorticity. This is a very significant source of acoustic damping; in fact, it is comparable in magnitude to other important damping mechanisms in unstable combustors (such as radiation out of the exhaust nozzle) (Zinn 1972).

In closing, it should be noted that although excitation of vorticity has significant effects on flame–acoustic interactions, the excitation of entropy does not. To the order of approximation considered in this analysis, entropy fluctuations are forced disturbances and do not interact with the acoustic field. The acoustic field only couples with the entropy mode through terms of $O(M\eta)^2$ and higher.

4. Summary and conclusions

This paper has described an analysis of the leading-order processes that control the interactions between flames and acoustic waves in a simplified geometry. The principal conclusions of this analysis are: (i) the amount of acoustic energy produced or dissipated at the flame depends upon the angle of the incident wave, Θ, the flame speed Mach number, M_{x1}, the temperature jump across the flame, Λ, the ratio of specific heats, γ, and the flame speed response parameter, κ; (ii) fluctuations of the flame speed by chemical kinetic processes have significant effects upon the acoustic energy produced by the flame; and (iii) the baroclinic production of vorticity by acoustic waves acts as a significant source of acoustic damping. It has also been shown that the net acoustic energy produced by these interactions is determined by two competing processes: (i) energy addition by unsteady heat release processes due to the unsteady flux of unburned reactants through the flame by either fluctuations in the flame speed or density of the unburned reactants; (ii) energy dissipation by the transfer of acoustic energy into the vorticity mode. While these results emphasize the role of these processes in understanding the studied interactions, it should be pointed out that other processes not captured in this model problem (such as flame area fluctuations, or strain-induced flame speed fluctuations) are also anticipated to introduce potentially significant new effects. As such, it is suggested that the following two generalizations would be useful in applying these results to more realistic geometries; (i) analyses of the response of non-planar flames to acoustic disturbances; and (ii) the response of flames to the more complex (i.e. non-planar) acoustic fields typically encountered in practice.

We close by noting that the second generalization can, to some extent, be examined by a straightforward application of the above results. Since attention is restricted to a linear analysis, the response of the flame to a number of waves with arbitrary phases, orientations, and magnitudes can be determined by superposition of the solutions presented in the previous section. Such a technique is analogous to that described by Brekhovskikh (1980) to analyse the response of beams or membranes to complex acoustic fields, i.e. the response of the structure to a plane wave is determined and then the appropriate combination of plane waves is superposed to determine the structure's response to an arbitrary acoustic field. Thus, the energy produced by the flame in response to m simultaneous waves originating from upstream with amplitudes A_i and l waves originating from downstream with amplitude B_i is

$$\frac{\langle \Delta I_a \rangle}{\langle I_{a,incident} \rangle} = 4(\Lambda - 1)M_{x1}$$

$$\times \frac{\mathrm{Re}\left(\sum_{j=1}^{m} \tilde{A}_j + \sum_{j=1}^{l} \tilde{B}_j\right)\left(\sum_{j=1}^{m} \tilde{A}_j E_j^1 + \sum_{j=1}^{l} \tilde{B}_j E_j^2\right)^*}{\mathrm{Re}\left(\sum_{j=1}^{m} A_j + \sum_{j=1}^{l} B_j\right)\left(\sum_{j=1}^{m} A_j \sqrt{1 - \sin^2 \Theta_j} + \sum_{j=1}^{l} B_j \sqrt{\Lambda(1 - \sin^2 \Theta_j)}\right)^*}, \quad (29)$$

where Re and the superscript * denote the real part and complex conjugate, respectively, and

$$\left.\begin{aligned} \tilde{A}_j &= \frac{A_j}{1 + \sqrt{\Lambda(1 - \Lambda \sin^2 \Theta_j)/(1 - \sin^2 \Theta_j)}}, \\ \tilde{B}_j &= \frac{B_j}{1 + \sqrt{(1 - \sin^2 \Theta_j/\Lambda)/(\Lambda(1 - \sin^2 \Theta_j))}}, \\ E_j^1 &= 2 - \gamma + \gamma\kappa - \Lambda \sin^2 \Theta_j, \quad E_j^2 = 2 - \gamma + \gamma\kappa - \sin^2 \Theta_j. \end{aligned}\right\} \quad (30)$$

This research was partially supported by AGTSR under contract 95-01-SR031.

REFERENCES

BREKHOVSKIKH, L. M. 1980 *Waves in Layered Media*. Academic.

CHU, B. T. 1953 On the generation of pressure waves at a plane flame front. *Fourth Symp. (Intl) on Combustion*, pp. 603–612. The Combustion Institute.

CHU, B. T. & KOVASNAY, L. S. G. 1958 Nonlinear interactions in a viscous, heat conducting. compressible gas. *J. Fluid Mech.* **3**, 494–514.

CLAVIN, P. 1985 Dynamic behavior of premixed flame fronts in laminar and turbulent flows. *Prog. Energy Combust. Sci.* **11**, 1–59.

COHEN, J. & ANDERSON, T. 1996 Experimental investigation of near-blowout instabilities in a lean premixed combustor. *AIAA Paper* 96-0819.

DOWLING, A. P. 1999 A kinetic model of a ducted flame. *J. Fluid Mech.* **394**, 51–72.

FLEIFEL, M., ANNASWAMY, A. M., GHONIEM, Z. A. & GHONIEM, A. F. 1996 Response of a laminar premixed flame to flame oscillations: a kinematic model and thermoacoustic instability results. *Combust. Flame* **106**, 487–510.

LIEUWEN, T. 1999 Investigation of combustion instability mechanisms in premixed gas turbines. PhD Thesis, Georgia Institute of Technology.

LIEUWEN, T. & ZINN B. T. 1998*a* Application of boundary element methods in modeling multidimensional flame-acoustic interactions. In *Boundary Elements XX* (A. Kassab, C. A. Brebbia & M. Chopra). Computational Mechanics Publications.

LIEUWEN, T. & ZINN B. T. 1998*b* The role of equivalence ratio oscillations in driving combustion instabilities in low NO_x gas turbines. *Twenty Seventh Symp. (Intl) on Combustion*, pp. 1809–1816. The Combustion Institute.

MARBLE, F. E. & CANDEL, S. M. 1978 An analytical study of the non-steady behavior of large combustors. *Seventeenth (Intl) Symp. on Combustion*, pp. 761–769. The Combustion Institute.

MARKSTEIN, G. H. 1964 Theory of flame propagation. In *Nonsteady Flame Propagation* (ed. G. H. Markstein). Pergamon.

MCINTOSH, A. C. 1991 Pressure disturbances of different length scales interacting with conventional flames. *Combust. Sci. Tech.* **75**, 287–309.

METGHALCHI. M. & KECK, J. C. 1982 Burning velocities of mixtures of air with methanol, isooctane, and indolene at high pressure and temperature. *Combust. Flame* **48**, 191–210.

PERACCHIO, A. A. & PROSCIA, W. M. 1998 Nonlinear heat release acoustic model for thermo–acoustic instability in lean premixed combustors. *ASME Paper* 98-GT-269.

PIERCE, A. D. 1991 *Acoustics: An Introduction to its Physical Principles and Applications*. Acoustical Society of America.

POINSOT, T. & CANDEL, S. M. 1988 A nonlinear model for ducted flame combustion instabilities. *Combust. Sci. Tech.* **61**, 121–153.

SUBBAIAH, M. V. 1983 Nonsteady flame spreading in two dimensional ducts. *AIAA J.* **21**, 1557–1564.

YANG, V. & CULICK, F. E. C. 1983 Linear theory of pressure oscillations in liquid-fueled ramjet engines. *AIAA Paper* 83-0574.

ZINN, B. T. 1972 Longitudinal mode acoustic losses in short nozzles. *J. Sound Vib.* **22**, 93–105.